Engineering Mathematics
2025, Vol. 9, No. 2, pp. 31–44
https://doi.org/10.11648/j.engmath.20250902.12

Research Article

Parameter Identification of Fractional-order Systems with Unknown Both State and Input Delays Based on Block Pulse Functions

Yu-Gang Hyon[1], Hyon-Ju Sin[1], Myong-Hyok Sin[1,*], Chol Min Sin[2], Hun Kim[1]

[1]Faculty of Mathematics, Kim Il Sung University, Pyongyang, Democratic People's Republic of Korea
[2]Institute of Mathematics, State Academy of Sciences, Pyongyang, Democratic People's Republic of Korea

Abstract

In this paper, we propose a method for identification of continuous-time fractional-order systems with unknown states and input delays. In practice, many systems are modeled accurately with fractional differential equations. In particular, many systems are modeled as fractional differential equations with input delay and state delay. Since the geometric and physical meaning of fractional calculus is not clear, it is difficult to model the real system directly to fractional order systems based on mechanical analysis. Thus, the identification of fractional order systems is the main method for constructing fractional order models and is the subject of the main research by many scientists. To solve the identification problem of systems with input delay and state delay, we use the fact that the fractional integral operator matrix by the block pulse functions is an upper triangular Toeplitz matrix. We have presented an efficient method to identify the linear and nonlinear parameters separably by using the commutativity and nilpotent property for multiplication between upper triangular Toeplitz matrices. We also have presented an efficient algorithm to newly approximate the Jacobian of the variable projection functional to solve the least squares problem with nonlinear parameters. Several simulation examples have been used to verify the effectiveness of the proposed method. It is shown that the input delay and the state delay have a significant effect on the output characteristics of the system, especially the state delay has a larger effect than the input delay.

Keywords

Block Pulse Function, Delay, Fractional Order System, Operational Matrix, Parameter Identification

1. Introduction

Due to non-local and historical memory properties of fractional order system (FOS), it has been widely studied by many researchers, see [1-7]. See also books [8-10].

The time delay is one of the natural problem in the practical engineering applications. FOSs with time delays can be found in various engineering systems such as chemical process, nuclear reactor, and the dynamic behavior of HIV infection of CD^+ T-cells, see [11]. In practice, FOSs with state delays arise from the dynamic behavior of viscoelastic materials, dynamical processes in self-similar and porous structures, control theory of mechanical system, strongly porous materials, some amorphous semiconductors, see [12-18]. In particular,

*Corresponding author: MH.Sin@star-co.net.kp (Myong-Hyok Sin)

Received: 27 October 2025; **Accepted:** 22 November 2025; **Published:** 29 December 2025

they arise from communication lags, feedback delay in measurement, delay in closed loop systems. In [17], the authors studied the control problem of SISO system which is presented as FOS with state delay when there exists a time delay in the state feedback loop. In [18], the authors use the control signal composed of state delay signals to stabilize the vibration system of single degree of freedom. The stabilization of FOSs is greatly affected by state delay, see [13, 16]. So this is an important non-negligible factor in the construction of model for FOS with state delay.

Because of the lack of acceptable geometric or physical explanations of fractional calculus, the identification for FOSs has been the best approach for building fractional order models of physical systems.

It is well known that the time domain identification method is one of the identifications of FOSs. This is based on the minimization of both equation error and output error and hence several least square algorithms have been used. For example, we refer to a recursive error prediction approach [19], modulating function method [20, 21], Haar wavelet-based method [22, 23], Block pulse functions (BPFs)-based method [11, 24-28].

Due to the simplicity of BPFs, the identification method using BPFs has been considered as an effective one to avoid the complicated and costly computations of the fractional derivatives of input and output signals.

In [11], to identify FOS with input delay, the fmincon function in MATLAB optimization toolbox was used to solve the optimization problem for determining both linear and nonlinear parameters. In the paper, the identification accuracy is sensitively varied according to the change of initial value. In general, the identification method for the linear continuous FOS which can estimate the linear and nonlinear parameters individually is considered as an efficient one having the independence of identification accuracy to initial condition and reducing the amount of work. In the context, we proposed an efficient identification method for FOS with both nonzero initial value and time delay, in which the linear and nonlinear parameters are individually estimated [28].

Within our knowledge, for FOSs with state delay there seems to be no work concerning parameter identification method in which linear and nonlinear parameters are individually estimated. So the aim of this paper is to develop such an identification method for FOSs with unknown state and input delays. The main novelty is to derive a new method, by which the linear and nonlinear parameters are separably estimated by using the commutativity and nilpotent property of the fractional integral operational matrix (FIOM) of BPFs. Moreover, we propose an efficient algorithm based on a new approximation about the Jacobian of variable projection functional for solving the least squares method for nonlinear parameters. With the estimated nonlinear parameters, we use the bias compensated recursive least squares (BCRLS) method in order to reduce the amount of work and get a high accuracy in the identification of linear parameters.

Simulation results show that in the proposed methods the unknown state and input delays, coefficients are efficiently identified.

The paper consists of 5 sections. In section 2, we give the definitions of fractional calculus, BPFs and explain the commutativity and nilpotent property of the FIOM of BPFs, which is upper triangular Toeplitz. Section 3 is devoted to construction of a separable recursive model for FOSs with unknown state and input delays, and of a method in which the least square problem including all parameters is projected onto the one only including nonlinear parameters, i.e., state and input delays. In section 4, we give some simulation examples for verifying the effectiveness of the proposed method. Section 5 concludes this paper.

2. Preliminaries

2.1. Definitions of the Fractional Order Integral and Derivative

The Riemann-Liouville fractional order integral is defined by

$$ {}_{t_0}^{R}I_t^{\alpha} f(t) := \frac{1}{\Gamma(\alpha)} \int_{t_0}^{t} (t-s)^{\alpha-1} f(s)ds, \tag{1} $$

where $\alpha > 0$, (t_0, t) is the integral interval and $\Gamma(\cdot)$ is the Gamma function, that is, $\Gamma(\alpha) := \int_0^{\infty} x^{\alpha-1} e^{-x} dx$.

For the sake of simplicity, we set $t_0 = 0$ and denote ${}_{t_0}^{R}I_t^{\alpha}$ by I^{α}.

Let $\ell \in \mathbb{N}, \ell - 1 < \alpha < \ell$. Then the Riemann-Liouville fractional order derivative is defined as

$$ \begin{aligned} D^{\alpha} f(t) &= I^{-\alpha} f(t) = D^{\ell} I^{\ell} I^{-\alpha} f(t) = D^{\ell} I^{\ell-\alpha} f(t) \\ &= \frac{d^{\ell}}{dt^{\ell}} \left[\frac{1}{\Gamma(\ell-\alpha)} \int_{t_0}^{t} (t-s)^{-\alpha+\ell-1} f(s) ds \right]. \end{aligned} \tag{2} $$

2.2. The FIOM of BPFs

As in [29], a set of BPFs in the semi-open interval $[0, T)$ is defined by

$$ B_n(t) := \begin{cases} 1, \frac{n-1}{N} T \le t < \frac{n}{N} T, \\ 0, otherwise, \end{cases} \tag{3} $$

where $n = 1, \cdots, N$, and N is the number of BPFs in the set.

We call $B(t) := [B_1(t), \cdots, B_N(t)]^T$ by block pulse vector. If we define the elements of $X = [x_1, \ldots, x_N]^T$ by

$$ x_n = \frac{N}{T} \int_{\frac{n-1}{N}T}^{\frac{n}{N}T} x(t)dt \approx x(\tfrac{n-1}{N}T), $$

then any absolute integrable function defined on interval $[0, T)$ can be approximated by a linear combination of BPFs as follow:

$$x(t) = \sum_{n=1}^{N}\left[\frac{N}{T}\int_{\frac{n-1}{N}T}^{\frac{n}{N}T} x(t)dt\right]B_n(t) \approx \sum_{n=1}^{N} x_n B_n(t) = X^T B(t). \tag{4}$$

By Eq. (1), we have

$$I^\alpha B(t) = \frac{1}{\Gamma(\alpha)} t^{\alpha-1} * B(t), \tag{5}$$

where the symbol $*$ means convolution. In [30], it was shown that Eq. (5) can be represented as

$$I^\alpha B(t) \approx P_\alpha B(t), \tag{6}$$

where

$$P_\alpha := \frac{h^\alpha}{\Gamma(\alpha+2)}\begin{pmatrix} \xi_1 & \xi_2 & \xi_3 & \cdots & \xi_N \\ 0 & \xi_1 & \xi_2 & \cdots & \xi_{N-1} \\ 0 & 0 & \xi_1 & \cdots & \xi_{N-2} \\ \cdots & \cdots & \cdots & \cdots & \cdots \\ 0 & 0 & 0 & 0 & \xi_1 \end{pmatrix}, \tag{7}$$

$$h = \frac{T}{N}, \xi_1 = 1, \xi_l = l^{\alpha+1} - 2(l-1)^{\alpha+1} + (l-2)^{\alpha+1}, l = 2, \ldots, N.$$

We call the matrix P_α by FIOM for BPFs. By Eqs. (4), (6), the fractional order integral of the function $x(t)$ is given by

$$I^\alpha x(t) \approx X^T P_\alpha B(t). \tag{8}$$

2.3. Commutativity and Nilpotent Property of the FIOM

By Eq. (4), the function $x(t-\tau)$ is expanded by BPFs as follow:

$$x(t-\tau) \approx X^T B(t-\tau) = \sum_{i=1}^{N} x_i B_i(t-\tau), \tag{9}$$

where

$$x_i = \frac{1}{h}\int_0^T x(t-\tau)B_i(t-\tau)dt. \tag{10}$$

In [11], it was pointed out that for $\tau = kh$, the delayed function $B(t-\tau)$ is represented as

$$B(t-\tau) = E_k \cdot B(t), t > \tau, 0 \le t \le T, \tag{11}$$

where for the Kronecker delta function δ_{ij}

$$E_k = \left(\delta_{i,j+k}\right)_{i,j=1}^{n}, k = 0,1,\cdots,n-1. \tag{12}$$

The matrix E_k is called k order delay operational one. In [28], it was shown that for non-negative integers i, j,

$$E_i E_j = E_j E_i = \begin{cases} I, \text{if } i+j=0 \\ E_{i+j}, \text{if } i+j<N \\ 0, \text{if } i+j \ge N. \end{cases} \tag{13}$$

As in [11], the Riemann-Liouville fractional order integral $B(t-\tau)$ is rewritten as

$$(I^\alpha B)(t-\tau) \approx P_\alpha B(t-\tau) = P_\alpha E_k B(t). \tag{14}$$

By Eq. (12), the FIOM from Eq. (7) is decomposed into

$$P_\alpha = \sum_{i=0}^{N-1} \frac{h^\alpha}{\Gamma(\alpha+2)} \xi_{i+1} E_i. \tag{15}$$

From Eq. (15), we can see that the FIOM from Eq. (7) is upper triangular Toeplitz which belongs to the subspace $T_N = \mathrm{Span}\{E_0, E_1, \cdots, E_{N-1}\}$.

Next, let us consider the commutativity of FIOMs. In the Appendix A below, we show the following properties: for any two FIOMs, $A, B \in T_N$ and $i, j = 0,1,2,\cdots$,

$$\begin{aligned} &\text{i) } A^i B^j \in T_N, \\ &\text{ii) } A^i B^j = B^j A^i, \\ &\text{iii) } (AB)^i = A^i B^i. \end{aligned} \tag{16}$$

In [31], it was shown that if a matrix A belongs to the strict upper triangular Toeplitz space $ST_N = \mathrm{Span}\{E_1, \cdots, E_{N-1}\}$, then A is nilpotent. Indeed, if $A \in ST_N$, then by (13) for all $k (\ge N)$

$$A^k = 0. \tag{17}$$

Remark 1 *Eq. (17) is the main key in the transformation of identification of FOS with state delay onto the separable least square problem. In particular, by Eqs. (16) and (17), we get that for* $B = \sum_{k=0}^{N-1} b_{k+1}E_k \in T_N$ *and* $Q = \sum_{k=1}^{N-1} b_{k+1}E_k$,

$$B^{-1} = (b_1 I + Q)^{-1} = \sum_{k=0}^{N-1} \frac{Q^k}{(-b_1)^{k+1}}. \tag{18}$$

For more detail, we refer to Appendix B.

3. Identification Algorithm for FOSs with Unknown State and Input Delays

Here we construct a new identification algorithm for FOSs with unknown state and input delays using separable least square problem. At first, the identification method is proposed for FOS from [14] and then for FOS from [12, 13, 16].

3.1. Case 1

Let us consider the FOS from [14]

$$D^{\alpha}x(t)+ax(t-\tau_a)=bu(t-\tau_b),\quad y(t)=x(t)+w(t), \tag{19}$$

where $\tau_a=kh,\tau_b=lh$ and N is the number of BPFs and T is the simulation time, and $u(t),x(t),y(t),w(t)$ are input signal, state, output signal and the Gauss white noise, respectively.

From Eqs. (8) and (14) the first equation in Eq. (19) can be rewritten as

$$X^T(I+aP_{\alpha}E_k)B(t)=bU^TP_{\alpha}E_lB(t).$$

Hence by (4)

$$x(t)=bU^TP_{\alpha}E_l(I+aP_{\alpha}E_k)^{-1}B(t). \tag{20}$$

By Eq. (18), the matrix $(I+aP^{\alpha}E_k)^{-1}$ with $k\geq 1$ is the following:

$$(I+aP_{\alpha}E_k)^{-1}=\sum_{i=0}^{N-1}(-1)^i a^i P_{\alpha}^i E_{ki}. \tag{21}$$

Inserting Eq. (21) into Eq. (20) implies that

$$x(t)=bU^TP_{\alpha}E_l\left[\sum_{i=0}^{N-1}(-1)^i a^i P_{\alpha}^i E_{ki}\right]B(t). \tag{22}$$

Now we set

$$\theta_L=(\theta_1,\theta_2,\cdots,\theta_N)^T,\theta_i=(-1)^{(i-1)}ba^{(i-1)},\theta_{NL}=(k,l)^T,$$

$$\varphi(\theta_{NL},t)=\left(U^TP_{\alpha}E_lB(t),U^TP_{\alpha}^2E_{(k+l)}B(t),U^TP_{\alpha}^3E_{(2k+l)}B(t),\cdots,U^TP_{\alpha}^NE_{((N-1)k+l)}B(t)\right)_{(1\times N)}.$$

If $Mk+l<N\leq(M+1)k+l$, then by the previous notation Eq. (22) can be rewritten as

$$x(t)=\varphi(\theta_{NL},t)\theta_L, \tag{23}$$

where

$$\varphi(\theta_{NL},t)=\left(U^TP_{\alpha}E_lB(t),U^TP_{\alpha}^2E_{(k+l)}B(t),\cdots,U^TP_{\alpha}^{(M+1)}E_{(Mk+l)}B(t),0,\cdots,0\right). \tag{24}$$

Remark 2 *In the estimation of the nonlinear parameter $\theta_{NL}=(k,l)^T$, for $\tau_a,\tau_b\in[\tau_{min},\tau_{max}]$ or $k,l\in[i_{min},i_{max}]$, only the first up to $M+1=[N/i_{min}]$ elements in Eq. (24) can be non-zero. The greater k and l, the smaller the amount of work.*

By Eq. (24) the data matrix $\Phi(\theta_{NL})$ for N sampling points can be written as

$$\Phi(\theta_{NL})=\{\varphi_{ij}(\theta_{NL})\}_{N\times N}, \tag{25}$$

where

$$\varphi_{ij}(\theta_{NL})=\begin{cases}U^TP_{\alpha}^jE_{(j-1)k+l}B(i), \text{if } i=1,\cdots,N, j=1,\cdots,M+1,\\ 0, \text{if } j>M+1.\end{cases} \tag{26}$$

Then by Eqs. (25) and (26) the identification for (19) is reduced to the separable least square problem as

$$R(\theta_L,\theta_{NL})=\|Y-\Phi(\theta_{NL})\theta_L\|_2^2:\min, \tag{27}$$

where Y is sampling value vector for $y(t)$.

3.2. Case 2

Let us consider the FOS from [12, 13, 16]

$$D^{\alpha}x(t)+a_1x(t-\tau_a)+a_0x(t)=bu(t-\tau_b),\quad y(t)=x(t)+w(t), \tag{28}$$

where $\tau_a=kh,\tau_b=lh,N,T,u(t),x(t),y(t),w(t)$ are the same as in the FOS (19).

From Eq. (8) we can rewrite Eq. (28) as

$$X^T(I+a_1P_{\alpha}E_k+a_0P_{\alpha})B(t)=bU^TP_{\alpha}E_lB(t).$$

Hence

$$x(t)=bU^TP_{\alpha}E_l(I+a_1P_{\alpha}E_k+a_0P_{\alpha})^{-1}B(t). \tag{29}$$

From (18) and Appendix C, the matrix $(I+a_1P^{\alpha}E_k+a_0P_{\alpha})^{-1}$ with $k\geq 1$ can be rewritten as

$$(I+a_1P_{\alpha}E_k+a_0P_{\alpha})^{-1}=\sum_{n=0}^{N-1}c_1c_2^nD_{\alpha}(c_3,k,n), \tag{30}$$

where $c_1:=\frac{1}{1+a_0f_1},c_2:=\frac{a_1}{1+a_0f_1},c_3:=\frac{a_0}{a_1},D_{\alpha}(c_3,k,n):=\sum_{i=0}^{n}c_3^{n-i}E_{ik}S_{\alpha}(n,i)$. Once α is known, the matrix $S_{\alpha}(n,i)$ is represented as

$$S_\alpha(n,i) = \binom{n}{i} P_\alpha^i (P_\alpha - (\alpha+2)\xi_1 I)^{n-i}.$$

Remark 3 *If* $|c_3| \leq 1$, *then the convergence of proposed algorithm is guaranteed with increase of the number of BPFs. If* $|c_3| > 1$, *then in Appendix C we can set* $a_1/a_0 = c_3$ *and modify the algorithm.*

Inserting (30) into (29) implies that

$$x(t) = bU^T P_\alpha E_l \sum_{n=0}^{N-1} (-1)^n c_1 c_2^n D_\alpha(c_3,k,n) B(t). \quad (31)$$

If $\theta_n = (-1)^n b c_1 c_2^n, n = 0,1,\cdots,N-1$, in Eq. (31), then $\theta_L = (\theta_0,\theta_1,\cdots,\theta_{N-1})^T$ is the linear parameter and $\theta_{NL} = (c_3,k,l)^T$ the nonlinear parameter. Then Eq. (31) can be rewritten as

$$x(t) = \varphi(\theta_{NL},t)\theta_L, \quad (32)$$

where

■(φ(θ_NL, t) = &(U^T P_α E_l D_α (c_3, k, 0)B(t), ⋯,

U^T P_α E_l D_α (c_3, k, n)B(t), @& ⋯,

U^T P_α E_l D_α (c_3, k, N − 1)B(t)).) (33)

By Eq. (32) the data matrix $\Phi(\theta_{NL})$ for N sampling points can be rewritten as

$$\Phi(\theta_{NL}) = \{\varphi_{ij}(\theta_{NL})\}_{N\times N}, \quad (34)$$

where

$$\varphi_{ij}(\theta_{NL}) = U^T P_\alpha E_l D_\alpha(c_3,k,j-1)B(i), i,j = 1,\cdots,N. \quad (35)$$

Thus from Eqs. (31) and (34) the identification for the FOS (28) is reduced to the separable least square problem

$$R(\theta_L,\theta_{NL}) = \|Y - \Phi(\theta_{NL})\theta_L\|_2^2 : \min, \quad (36)$$

where Y is the sampling value vector of $y(t)$.

3.3. Identification Algorithm

3.3.1. Identification Algorithm for Nonlinear Parameter

As we can see in Eqs. (27) and (36), the identifications for FOSs (19) and (28) with both state and input delays are reduced to the separable least square problem.

As [32], given the nonlinear parameter θ_{NL}, the solution of the optimization problem (27) and (36) for obtaining the linear parameters is

$$\theta_L = \Phi^+(\theta_{NL})Y, \quad (37)$$

where $\Phi^+(\theta_{NL}) = [\Phi^T(\theta_{NL})\Phi(\theta_{NL})]^{-1}\Phi^T(\theta_{NL})$ is Moore-Penrose pseudo-inverse.

Inserting Eq. (37) into Eq. (27) or (36) yields that we have the following optimization for nonlinear parameter θ_{NL}:

$$R_1(\theta_{NL}) = \left\|\left(I - P(\theta_{NL})\right)Y\right\|^2 : \min, \quad (38)$$

where $P(\theta_{NL}) = \Phi(\theta_{NL})\Phi^+(\theta_{NL}) \in \mathbb{R}^{N\times N}$ and

$$f(\theta_{NL}) := \left(I - P(\theta_{NL})\right)Y \quad (39)$$

is a variable projection functional.

The matrix $\Phi^+(\theta_{NL})$ needs the inverse matrix $[\Phi^T(\theta_{NL})\Phi(\theta_{NL})]^{-1}$. However, the matrix $\Phi^T(\theta_{NL})\Phi(\theta_{NL})$ can be singular. To solve the problem, we follow the argument from [28].

If the matrix $\Phi^-(\theta_{NL})$ satisfies

$$\Phi(\theta_{NL})\Phi^-(\theta_{NL})\Phi(\theta_{NL}) = \Phi(\theta_{NL}), \left(\Phi(\theta_{NL})\Phi^-(\theta_{NL})\right)^T = \Phi(\theta_{NL})\Phi^-(\theta_{NL}), \quad (40)$$

then the matrix $P(\theta_{NL})$ from (38) can be rewritten as

$$P(\theta_{NL}) = \Phi(\theta_{NL})\Phi^-(\theta_{NL}). \quad (41)$$

Here the matrix $\Phi^-(\theta_{NL})$ can be obtained as follow: if $rank\Phi(\theta_{NL}) = r$, then the matrix $\Phi(\theta_{NL})$ is decomposed as

$$\Phi(\theta_{NL}) = \mathrm{G}\begin{pmatrix}\mathrm{U}_{11} & \mathrm{U}_{12} \\ 0 & 0\end{pmatrix}, \quad (42)$$

where $rankU_{11} = r, U_{11} \in \mathbb{R}^{r\times r}$ and U_{11} has normally orthonormal column vectors. Then the matrix

$$\Phi^-(\theta_{NL}) = \begin{pmatrix}\mathrm{U}_{11}^{-1} & 0 \\ 0 & 0\end{pmatrix} G^T$$

satisfies Eq. (40). Setting $G = [G_1, G_2], G_1 \in \mathbb{R}^{N\times r}$, we have

$$P(\theta_{NL}) = G_1 G_1^T. \quad (43)$$

Thus Eq. (38) is represented as

$$R_2(k) = \|(I - G_1 G_1^T)\mathrm{Y}\|^2 : \min. \quad (44)$$

As pointed out in [28], the matrix G_1 consists of the first linear independent r column vectors which are obtained by orthonormalizing $\Phi(\theta_{NL})$ by virtue of Gram-Schmidt orthogonalization.

In order to identify the nonlinear parameter based on Levenberg-Marquardt (LM) algorithm from [31], we have to construct the Jacobian for the cost functional (44).

Remark 4 *In this paper, we propose a new construction of Jacobian of variable projection functional, in which the* *matrix Φ^+ is no longer used.*

To this end, we first calculate the Jacobian of variable projection functional $f(\theta_{NL})$ from (39).

If $\theta_{NL} = (x_1, x_2, \cdots, x_m)^T$ for $m = 2$ or 3, then we have for $k = 1, \cdots, m$

$$\begin{aligned}\nabla_k f &= -(\nabla_k \Phi)\Phi^+ Y + \Phi[\nabla_k(\Phi^+)]Y = -(\nabla_k \Phi)\Phi^+ Y + \Phi\nabla_k[(\Phi^T\Phi)^{-1}\Phi^T]Y \\ &= -(\nabla_k \Phi)\Phi^+ Y + \Phi(\Phi^T\Phi)^{-1}[(\nabla_k\Phi)^T\Phi - \Phi^T(\nabla_k\Phi)](\Phi^T\Phi)^{-1}\Phi^T Y \\ &= -[\nabla_k\Phi + (\Phi^+)^T(\nabla_k\Phi)^T\Phi - \Phi\Phi^+(\nabla_k\Phi)]\Phi^+ Y.\end{aligned}$$

As [33] we can neglect the term $(\Phi^+)^T(\nabla_k\Phi)^T\Phi\Phi^+Y$ in the previous formula. This enables us to reduce the amount of work without a great affection about the approximation accuracy of Jacobian. By (43) we have

$$\begin{aligned}\nabla_k f &\approx -[\nabla_k\Phi - \Phi\Phi^+(\nabla_k\Phi)]\Phi^+Y = -(I - \Phi\Phi^+)(\nabla_k\Phi)\Phi^+Y \\ &= -(I - G_1G_1^T)(\nabla_k\Phi)\Phi^+Y.\end{aligned} \tag{45}$$

Since $\Phi^+Y = \Phi^+\Phi\theta_L = \Phi^+\Phi\Phi^-\Phi\theta_L = \Phi^-Y$ by (40) and (41), we have

$$\nabla_k f \approx -(I - G_1G_1^T)(\nabla_k\Phi)\Phi^-Y. \tag{46}$$

Moreover, $(\nabla_k\Phi)_{ij}, i, j = 1, \cdots, N$, can be obtained as follow: for the case 1 with $x_1 = k, x_2 = l$

$$\begin{aligned}(\nabla_1\Phi)_{ij} &\approx U^TP_\alpha^2E_{(j-1)(k+1)+l}B(i) - U^TP_\alpha^2E_{(j-1)k+l}B(i), \\ (\nabla_2\Phi)_{ij} &\approx U^TP_\alpha^2E_{(j-1)k+l+1}B(i) - U^TP_\alpha^2E_{(j-1)k+l}B(i),\end{aligned} \tag{47}$$

while for the case 2 with $x_1 = c_3, x_2 = k, x_3 = l$

$$\begin{aligned}(\nabla_1\Phi)_{ij} &= U^TP_\alpha E_l \frac{\partial}{\partial c_3}D_\alpha(c_3, k, j-1)B(i), \\ (\nabla_2\Phi)_{ij} &\approx U^TP_\alpha E_l D_\alpha(c_3, k+1, j-1)B(i) - U^TP_\alpha E_l D_\alpha(c_3, k, j-1)B(i), \\ (\nabla_3\Phi)_{ij} &\approx U^TP_\alpha E_{l+1} D_\alpha(c_3, k, j-1)B(i) - U^TP_\alpha E_l D_\alpha(c_3, k, j-1)B(i),\end{aligned} \tag{48}$$

where

$$\frac{\partial}{\partial c_3}D_\alpha(c_3, k, j-1) = \sum_{l=0}^{j-1}(j-2-l)c_3^{j-2-l}E_{lk}S_\alpha(j-1, l).$$

By Eqs. (47) and (48) the algorithm for determining the nonlinear parameter θ_{NL} is constructed as follow:

[Algorithm 1]

Step 1: Set $k = 0$ and select the initial point $\theta_{NL}(0)$ and admissible error $\varepsilon > 0$.

Step 2: Set $\theta_{NL}(k+1) = \theta_{NL}(k) + \lambda_k d_k$ and determine the scrutiny direction d_k as

$$\left[J(\theta_{NL}(k))^T J(\theta_{NL}(k)) + \lambda_k I\right] d_k = -J(\theta_{NL}(k))E(\theta_{NL}(k)),$$

where $E = (I - G_1G_1^T)Y$ is error function, λ_k damping factor. The Jacobian $J(\theta_{NL}(k))$ is determined by Eq. (45) as

$$J(\theta_{NL}(k)) = \left(\nabla_1 f(\theta_{NL}(k)),\ \nabla_2 f(\theta_{NL}(k)),\ \cdots,\ \nabla_m f(\theta_{NL}(k))\right),$$

where $m = 2$ for the case 1, while $m = 3$ for the case 3. The step size λ_k is determined by $\underset{\lambda\ge 0}{\mathrm{argmin}}\left\|\left(I - P(\theta_{NL}(k) + \lambda d_k)\right)\mathrm{Y}\right\|^2$.

Step 3: If $\left\|\left(I - P(\theta_{NL}(k+1))\right)\mathrm{Y}\right\|^2 < \varepsilon$, then we set $\hat{\theta}_{NL} = \theta_{NL}(k+1)$ and if not, then go to step 2 with $k = k + 1$.

3.3.2. Identification Algorithm for Linear Parameters

If the nonlinear parameter θ_{NL} is estimated by algorithm 1, the linear parameter θ_L can be estimated by Eq. (37).

Remark 5 *As mentioned above, the matrix $\Phi^+(\theta_{NL})$ does not exist if $\det[\Phi^T(\theta_{NL})\Phi(\theta_{NL})] = 0$. Moreover, it is pointed out in [25] that even though $\det[\Phi^T(\theta_{NL})\Phi(\theta_{NL})] \neq 0$, the linear parameter estimated by Eq. (37) has a deviation when there exists an output noise. Furthermore, increase of the number of BPFs yields increase of the number of the linear parameters, which makes it impossible for us to calculate them. Hence we use BCRLS method from [25].*

We select $t = (p-1)h, p = 1, \dots, N$, as sampling times and introduce the notations

$$X^TB(t) = X_1(p), X^TP_\alpha B(t) = X_0(p), U^TP_\alpha B(t) = U_0(p). \tag{49}$$

Then the FOS (19) or (28) can be rewritten as

$$X_1(p) = \varphi(p, \hat{k}, \hat{l})\theta_L, \tag{50}$$

where $\hat{k}, \hat{l}$ are the already estimated nonlinear parameters.

For the FOS (19), we have

$$\begin{aligned} &\varphi(p,\hat{k},\hat{l}) = [-X_0(p-\hat{k}), U_0(p-\hat{l})], \text{for } p = 1,\cdots,N \\ &\theta_L = (a,b)^T, \end{aligned} \tag{51}$$

and while for the FOS (28)

$$\begin{aligned} &\varphi(p,\hat{k},\hat{l}) = [-X_0(p-\hat{k}), -X_0(p), U_0(p-\hat{l})], \text{for } p = 1,\cdots,N \\ &\theta_L = (a_1, a_0, b)^T. \end{aligned} \tag{52}$$

Then the BCRLS for estimating linear parameters is the following:

[Algorithm 2]

$$\begin{cases} L(p,\hat{k},\hat{l}) = Q(p-1)\varphi(p,\hat{k},\hat{l})[\lambda + \varphi^T(p,\hat{k},\hat{l})Q(p-1)\varphi(p,\hat{k},\hat{l})]^{-1}, Q(0) = p_0 I, \\ \varepsilon(p,\hat{k},\hat{l}) = y(p) - \hat{\varphi}^T(p,\hat{k},\hat{l})\hat{\theta}_{RLS}(p-1), \\ \hat{\theta}_{RLS}(p,\hat{k},\hat{l}) = \hat{\theta}_{RLS}(p-1,\hat{k},\hat{l}) + L(p,\hat{k},\hat{l})\varepsilon(p,\hat{k},\hat{l}), \\ Q(p,\hat{k},l) = [I - L(p,\hat{k},\hat{l})\varphi^T(p,\hat{k},\hat{l})]Q(p-1,\hat{k})/\lambda, \\ \theta_{BCRLS}(p,\hat{k},\hat{l}) = \theta_{RLS}(p-1,\hat{k},\hat{l}) - Q(p,\hat{k},\hat{l})[\sum_{i=1}^{t} \varphi(i,\hat{k},\hat{l})(X_n(i) - \varphi^T(i,\hat{k},\hat{l})\theta_{RLS}(i,\hat{k},\hat{l}))], \end{cases} \tag{53}$$

where $Q(0) = \gamma I, \hat{\theta}_{RLS}(0) = (1/p_0,\cdots,1/p_0)^T$ and γ is a very large parameter which usually has the size of $(10^3 : 10^8)$ and $0.2 \le \lambda < 1$.

4. Simulation Examples

Example 1

We consider

$$\begin{aligned} &D^{\alpha}x(t) + ax(t-\tau_a) = bu(t-\tau_b), \\ &y(t) = x(t) + w(t), \end{aligned} \tag{54}$$

where $a = 1.1, b = 1.5, \tau_a = 1.2, \tau_b = 0.8, \alpha = 0.7$ and $w(t)$ is the Gauss white noise. The simulation time is $T = 20s$.

Figure 1 shows the step response for the FOS (54) with noise or without noise.

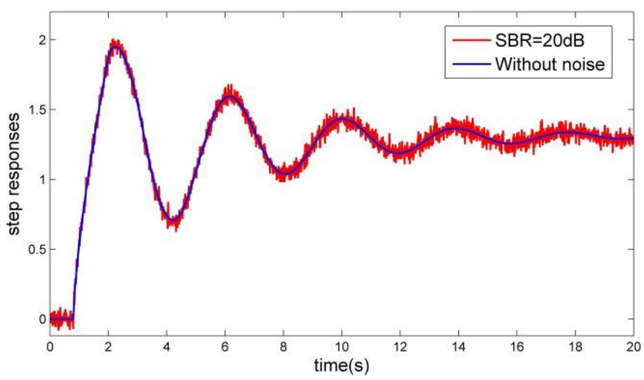

Figure 1. *The Step Response for Example 1.*

To show the dependence of output response to input or state delays, we present Figure 2.

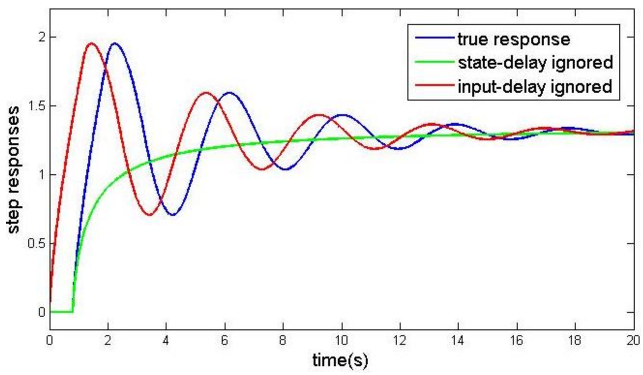

Figure 2. *The Step Response for Example 1 with Ignored State or Input Delay.*

As we can see in Figure 2, the output response for the system with ignored state delay is greatly different from real response than the one for the system with ignored input delay. This shows that the state delay is an important non-negligible factor.

Figure 3 shows the error function (44) for the FOS (54) without noise or with noise $SNR = 20dB$, in which the errors for state delay τ_a and input delay τ_b is presented in the range of $[0.2, 1.6]$.

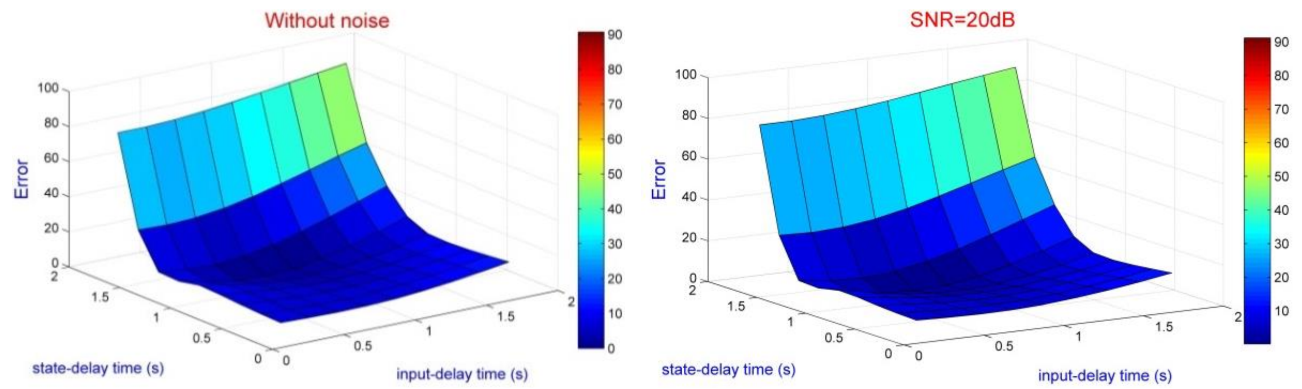

(a) Without Noise. (b) with Noise.

Figure 3*. The Error Function for FOS (54).*

Table 1 lists the identification results of nonlinear parameters τ_a, τ_b for the FOS (51) with noise or without noise. Here the algorithm 1 is used.

Table 1*. Identification Results of Nonlinear Parameters for Example 1.*

nonlinear parameter	true(s)	without noise	with noise (SNR)	
			10dB	20dB
state delay time	1.2	1.2000	1.2000	1.2000
input delay time	0.8	0.8000	0.8000	0.8000

Table 1 shows that if the state and input delay times are integer times of the sampling interval T/N, then there does not exist the identification error for nonlinear parameters.

Based on this identification result, we can estimate the linear parameters. Here we use algorithm 2.

In Figure 4, the online identification process of linear parameters for the FOS (54) with noise or without noise is presented.

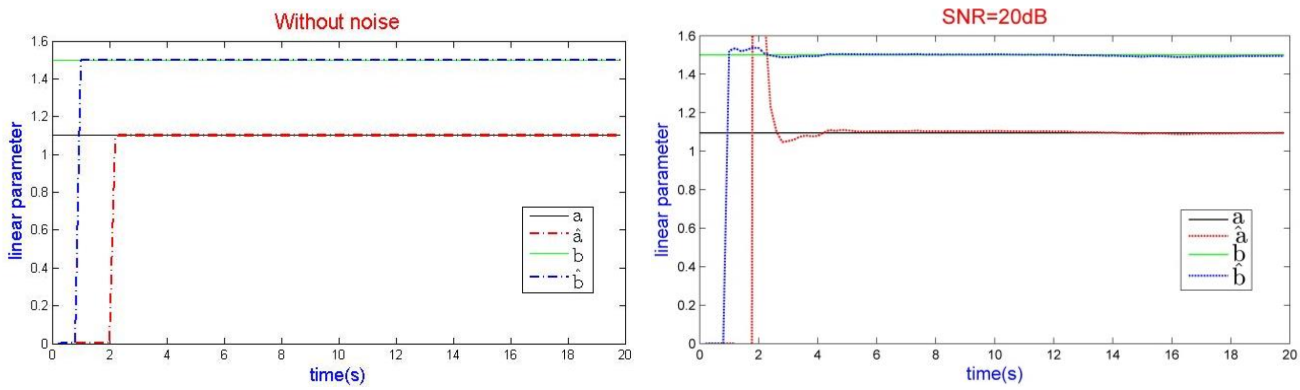

(a) Without Noise (b) with Noise

Figure 4*. The Identification Result for FOS (54).*

Table 2 shows the identification result according to various noise and numbers of BPFs. Table 2 represents the average values of 50 identification results obtained by using Monte-Carlo methods. In Table 2, we present the identification accuracy by the relative error between real parameter $\theta = (a, b)^T$ and estimated one $\hat{\theta} = (\hat{a}, \hat{b})^T$, i.e.,

$$\delta = \frac{\|\theta-\hat{\theta}\|}{\|\theta\|} \times 100(\%). \qquad (55)$$

Table 2. *The Identification Result According to Various Noise and Numbers of BPFs.*

linear parameter	true	BPFs' number =100			BPFs' number =500		
		SNR=10dB	SNR=20dB	SNR=50dB	SNR=10dB	SNR=20dB	SNR=50dB
a	1.1	1.1313	1.0898	1.1001	1.0986	1.0998	1.1000
b	1.5	1.6241	1.4997	1.4999	1.5014	1.5001	1.5000
δ	-	6.88	0.54	7.6e-03	0.100	0.010	0.000

From Table 2, we can see that the more increase the number of BPFs, the more improve the identification accuracy.

Figure 5 shows the online identification process of example 1 with ignored state delay or input delay. Here $SNR = 20dB$ and $N = 100$.

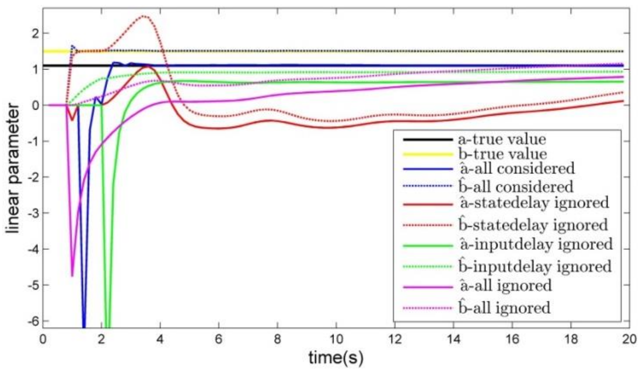

Figure 5. *The Dependence of Online Identification for Linear Parameters to Nonlinear Parameters.*

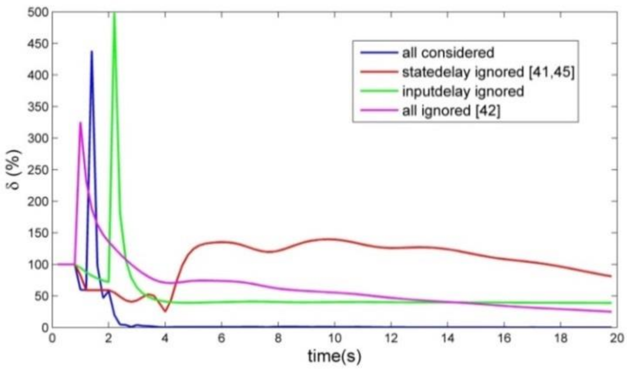

Figure 6. *The Dependence of Error Function to Nonlinear Parameters.*

In order to analyse the identification accuracy in more detail, we present the dependence of the function (55) to the nonlinear parameters, see Figure 6. Figure 6 shows that for FOS with both state and input delays, identification result of linear parameters is greatly different from the one for FOS with only input delay [11, 28], and without any delay [25]. In particular, the identification result is worse for FOS without state delay.

Example 2

We consider the system

$$\begin{aligned} &D^{\alpha}x(t) + a_1 x(t-\tau_a) + a_0 x(t) = bu(t-\tau_b), \\ &y(t) = x(t) + w(t), \end{aligned} \qquad (56)$$

where $a_1 = 2.5, a_0 =, b = 1..5, \tau_a = 1.2, \tau_b = 0.8, \alpha = 0.7$, $w(t)$ is the Gauss white noise and $T = 20s$.

Figure 7 shows the step response for the FOS (56) with noise or without noise.

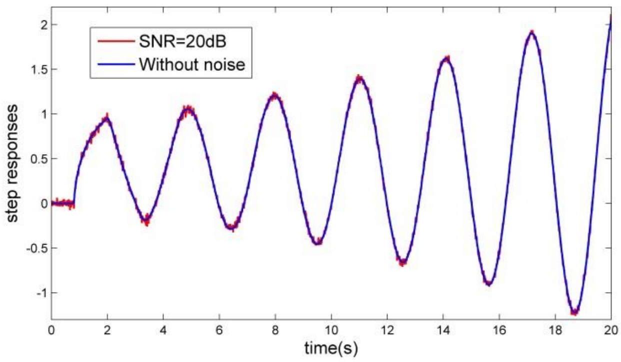

Figure 7. *The Step Response for Example 2.*

To show the dependence of output response to input or state delays, we present Figure 8.

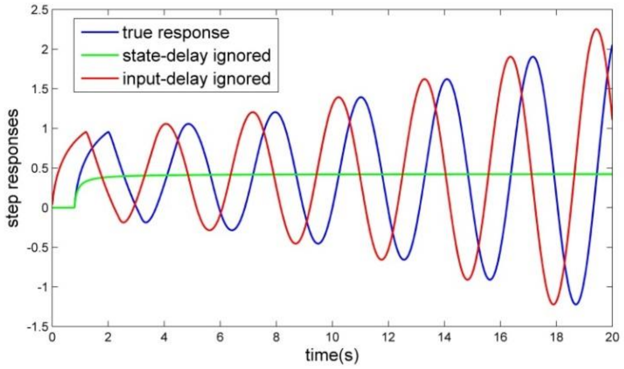

Figure 8. *The Step Response for Example 2 with Ignored State or Input Delay.*

As example 1, the output response for the system with ignored state delay is greatly different from real response than the one for the system with ignored input delay. This also shows that the state delay is an important non-negligible factor.

Figure 9 shows the error function (44) for the FOS (56) without noise or with noise $SNR = 20dB$ when $c_3 = 0.25$. Here the errors for state delay τ_a and input delay τ_b is presented in the range of $[0.2,1.6]$.

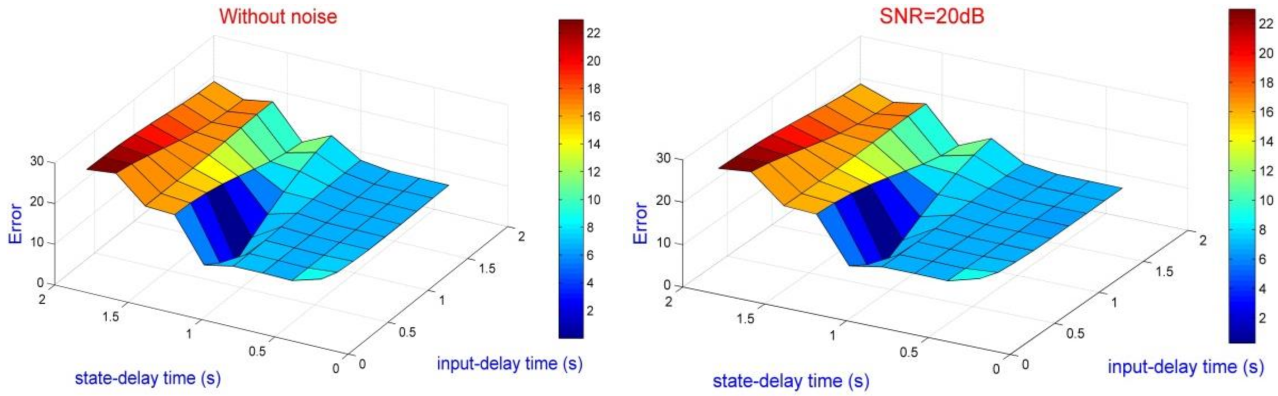

(a) Without Noise. (b) with Noise.

Figure 9. *The Error Function for FOS (56).*

From Figure 9 we can see that the error function (44) for the FOS (56) is seldom affected by the output noise.

Table 3 presents the identification results of nonlinear parameters τ_a, τ_b for the FOS (56) with noise or without noise.

Table 3. *Identification Results of Nonlinear Parameters for the FOS(56).*

nonlinear parameter	**true(s)**	**without noise**	**with noise**	
			SNR=10dB	**SNR=20dB**
state delay time	1.2	1.2000	1.2000	1.2000
input delay time	0.8	0.8000	0.8000	0.8000
auxiliary parameter	0.25	0.2500	0.2492	0.2501

Based on this identification result, we can estimate the linear parameters. Here we also use algorithm 2.

Figure 10 show the online identification process of linear parameters for the FOS (56) with noise or without noise.

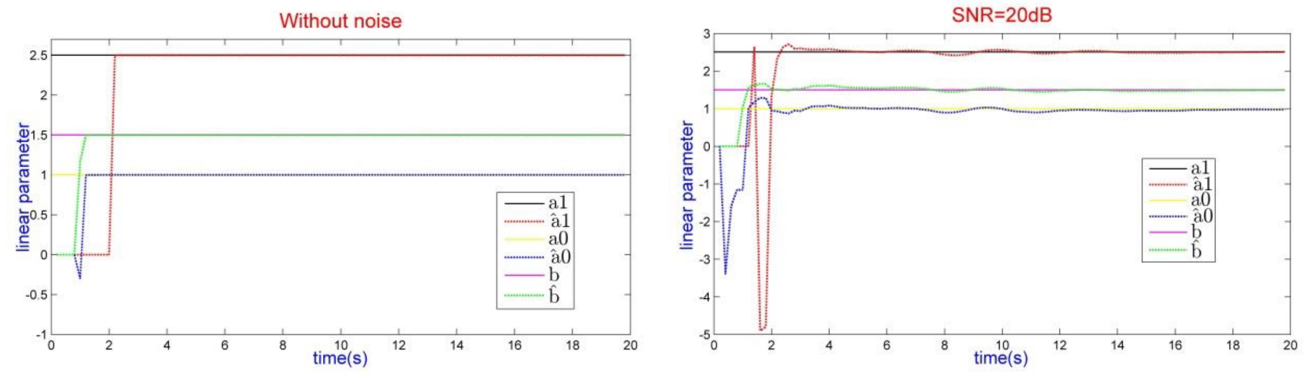

(a) Without Noise (b) with Noise.

Figure 10. *The Identification Result of Linear Parameters for FOS (56).*

Table 4 lists the identification result according to various noise and numbers of BPFs by the average values of 50 identification results obtained by using Monte-Carlo methods.

Table 4. *The Identification Result According to Various Noise and Numbers of BPFs.*

linear parameter	**true**	**BPFs' number =100**			**BPFs' number =500**		
		SNR=10dB	**SNR=20dB**	**SNR=50dB**	**SNR=10dB**	**SNR=20dB**	**SNR=50dB**
a_1	2.5	2.3909	2.4872	2.4997	2.4984	2.4999	2.5000
a_0	1.0	0.9670	1.1012	1.0054	1.0007	1.0003	1.0002
b	1.5	1.6103	1.5136	1.5019	1.5012	1.5001	1.5000
δ	-	5.1460	3.3388	1.7531	0.0687	0.0107	0.0064

From Table 4, we can see that the more increase the number of BPFs, the more improve the identification accuracy. Figure 11 shows the online identification process of example 2 with ignored state delay or input delay. Here $SNR = 20dB$ and $N = 100$.

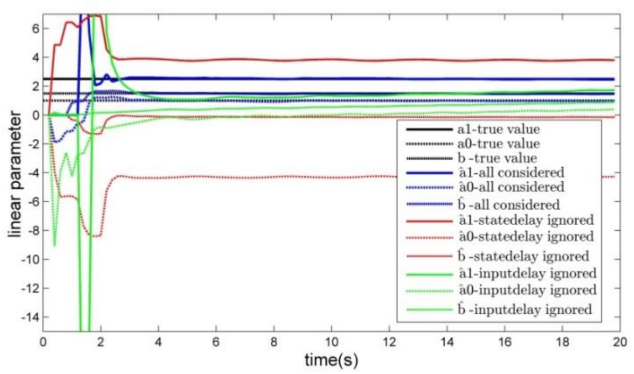

Figure 11. *The Dependence of Online Identification of Linear Parameters to Nonlinear Parameters.*

In Figure 12 the dependence of the function (55) to the nonlinear parameters is presented.

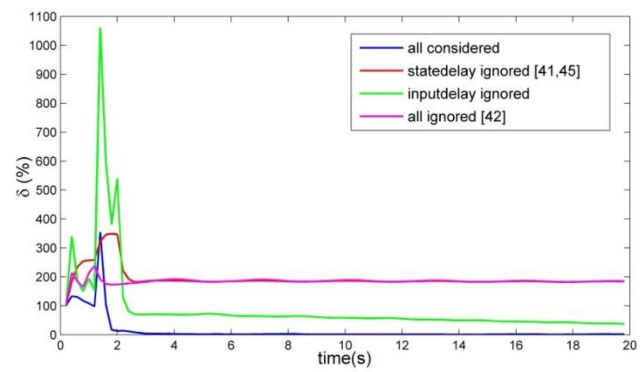

Figure 12. *The Dependence of Error Function to Nonlinear Parameters.*

From Figure 12 we can see that for linear continuous FOS, the identification accuracy of linear parameters is affected strongly by state delay than input delay and is nearly similar for the case of ignoring only state delay and the case of ignoring both state and input delay. Hence the state delay time must be estimated for linear continuous FOS with state delay.

5. Conclusion

In this paper, the identification method for linear continuous FOS with unknown state and input delays is proposed.

Simulation results show that the proposed method has a high identification accuracy for FOS with unknown state and input delays. In particular, Simulation result shows that the state delay is an important non-negligible factor.

Our further study is to develop an identification method for fractional order systems with unknown state and input delays, in which not only the delays and efficient but also differential order are estimated.

Abbreviations

FOS	Fractional Order System
BPF	Block Pulse Function
FIOM	Fractional Integral Operational Matrix
BCRLS	Bias Compensated Recursive Least Squares
LM	Levenberg-Marquardt

Author Contributions

Yu-Gang Hyon: Conceptualization, Writing – original draft

Hyon-Ju Sin: Data curation, Formal Analysis

Myong-Hyok Sin: Writing – original draft

Chol Min Sin: Data curation, Formal analysis, Writing – review & editing

Hun Kim: Validation, Software

Conflicts of Interest

The author declares no conflicts of interest.

Appendix

Appendix I: Proof of Eq. (16)

At first, let us prove i) in Eq. (16). Let $i = 2, j = 0$. Then

$$A^2 \in T_N. \tag{57}$$

By Eq. (15) we have $A = \sum_{k=0}^{N-1} a_{k+1} E_k$. Hence the matrix A^2 is represented as

$$A^2 = \sum_{p=1}^{N-1} \sum_{q=1}^{N-1} a_{p+1} a_{q+1} E_p E_q. \tag{58}$$

By Eq. (13), Eq. (58) can be rewritten as

$$A^2 = \sum_{p=0}^{N-1} \sum_{q=0}^{N-1} a_{p+1} a_{q+1} E_{p+q} = \sum_{k=0}^{N-1} c_{k+1} E_k,$$

where $0 \le k = p + q \le N - 1$, $c_{k+1} = \sum_{p=0}^{k} a_{p+1} a_{k-p+1}$. Thus Eq. (57) holds.

For $i = 1, j = 1$, we can follow the same argument to get

$$AB \in T_N, \tag{59}$$

where

$$AB = \sum_{p=0}^{N-1} \sum_{q=0}^{N-1} a_{p+1} b_{q+1} E_{p+q} = \sum_{k=0}^{N-1} d_{k+1} E_k, d_{k+1} = \sum_{p=0}^{k} a_{p+1} b_{k-p+1}. \tag{60}$$

By Eqs. (57) and (59) we have $A^i, B^j \in T_N$ and $A^i B^j \in T_N$.

It suffices to prove only $AB = BA$ for verifying ii) in Eq. (16). That $AB = BA$ is obvious by Eq. (60).

The validity of iii) in Eq. (16) follows immediately from ii).

Appendix II: Proof of Eq. (18)

Here we prove Eq. (18). We have

$$(b_1 I + Q) \sum_{k=0}^{N-1} \frac{Q^k}{(-b_1)^{k+1}} = \sum_{k=0}^{N-1} \frac{Q^k}{(-b_1)^k} + \sum_{k=0}^{N-1} \frac{Q^{k+1}}{(-b_1)^{k+1}} = \mathrm{I} + \frac{Q^N}{(-b_1)^N}.$$

On the other hand, $Q^N = 0$ by Eq. (17). Thus Eq. (18) is valid.

Appendix III: Proof of Eq. (30)

Here we prove Eq. (30). For simplicity, we set $f_i := \frac{h^\alpha}{\Gamma(\alpha+2)} \xi_i$. Direct calculations show that

■((I + a_1 P_α E_k + a_0 P_α)^(−1) = (I + a_1 P_α E_k + a_0 f_1 I + a_0 ∑_(i = 1)^(N − 1)▒ f_(i + 1) E_i)^(−1)@ = ((1 + a_0 f_1)I + a_1 P_α E_k + a_0 ∑_(i = 1)^(N − 1)▒ f_(i + 1) E_i)^(−1)@ = 1/(1 + a_0 f_1) (I + a_1/(1 + a_0 f_1) P_α E_k + a_0/(1 + a_0 f_1) ∑_(i = 1)^(N − 1)▒ f_(i + 1) E_i)^(−1).)

Using the result from Appendix A, we have for $k \neq 0$

$$(I + a_1 P_\alpha E_k + a_0 P_\alpha)^{-1} = \frac{1}{1+a_0 f_1} \sum_{n=0}^{N-1} (-1)^n \left(\frac{a_1}{1+a_0 f_1} P_\alpha E_k + \frac{a_0}{1+a_0 f_1} \sum_{i=1}^{N-1} f_{i+1} E_i \right)^n.$$

Now setting

$$c_1 := \frac{1}{1+a_0 f_1}, c_2 := \frac{a_1}{1+a_0 f_1}, c_3 := \frac{a_0}{a_1},\ Q_\alpha := \sum_{i=1}^{N-1} f_{i+1} E_i = P_\alpha - f_1 I,$$

we have

■((𝐼 + a_1 P_𝛼 E_k + a_0 P_𝛼)^(−1)& = c_1 ∑_(n = 0)^(N − 1)▒ (−1)^n c_2^n (P_𝛼 E_k + c_3 Q_𝛼)^n@& = c_1 ∑_(n = 0)^(N − 1)▒ (−1)^n c_2^n ∑_(i = 0)^n▒ (■(n@i)) c_3^(n − i) E_ik P_𝛼^i Q_𝛼^(n − i).)

Denoting $S_\alpha(n,i) := \binom{n}{i} P_\alpha^i Q_\alpha^{n-i}$ we obtain that

$$(I + a_1 P_\alpha E_k + a_0 P_\alpha)^{-1} = c_1 \sum_{n=0}^{N-1} (-)^n c_2^n \sum_{i=0}^{n} c_3^{n-i} E_{ik} S_\alpha(n,i).$$

In particular, there holds

$$S_\alpha(n,i) \in \mathrm{Span}\{E_0, E_1, \cdots, E_{N-1}\}, n = 0, \cdots, N-1, i = 0, \cdots, n.$$

On the other hand, setting

$$D_\alpha(c_3, k, n) := \sum_{i=0}^{n} c_3^{n-l} E_{ik} S_\alpha(n,i) =,$$

we have

$$D_\alpha(c_3, k, n) \in \mathrm{Span}\{E_0, E_1, \cdots, E_{N-1}\}, n = 0, \cdots, N-1,$$

and

$$(I + a_1 P_\alpha E_k + a_0 P_\alpha)^{-1} = \sum_{n=0}^{N-1} (-1)^n c_1 c_2^n D_\alpha(c_3, k, n).$$

Thus (30) is proved.

References

[1] W. Bauer, J. Baranowski, Fractional PIλD controller design for a magnetic levitation system, Electronics 9 (2020) paper no 2135, 15 pages.

[2] K. Oprzedkiewicz, M. Rosol, J. Zeglen-Wlodarczyk, The magnetic levitation system implementation of fractional-order PID controller, Electronics 10 (2021) paper no 524, 16 pages.

[3] C. I. Muresan, I. R. Birs, E. H. Dulf, D. Copot, L. Miclea, A review of recent advances in fractional-order sensing and filtering techniques, Sensors 21 (2021) paper no 5920, 26 pages.

[4] P. Torvik, R. Bagley, On the appearance of the fractional derivative in the behavior of real materials, J. Appl. Mech. 51 (1984) 294-298.

[5] J. Wang, L. Zhang, D. Xu, P. Zhang, G. Zhang, A simplified fractional order equivalent circuit model and adaptive online parameter identification method for Lithium-ion batteries, Mathematical Problems in Engineering 2019 (2019), 8 pages. https://doi/10.1155/2019/6019236

[6] L. Li, H. Zhu, A. Zhou, M. Hu, C. Fu, D. Qin, A novel online parameter identification algorithm for fractional-order equivalent circuit model of Lithium-ion batteries, Int. J. Electrochem. Sci. 15 (2020) 6863-6879.

[7] V. Erturk, P. Kumar, Solution of a COVID-19 model via new generalized Caputo-type fractional derivatives, Chaos, Solitons and Fractals 139 (2020). https://doi.org/10.1016/j.chaos.2020.110280

[8] V. V. Uchaikin, Fractional Derivatives for Physicists and Engineers: Volume I. Background and Theory, Nonlinear Physical Science, Higher Education Press and Springer-Verlag, Beijing and Berlin, 2013.

[9] R. Hilfer, Applications of Fractional Calculus in Physics, World Scientific, Singapore, 2000.

[10] S. Das, Functional Fractional Calculus for System Identification and Controls, Springer-Verlag, Berlin, Heidelberg, 2008.

[11] Y. Tang, N. Li, M. Liu, Y. Lu, W. Wang, Identification of fractional-order systems with time delays using block pulse functions, Mechanical Systems and Signal Processing 91 (2017) 382-394. http://dx.doi.org/10.1016/j.ymssp.2017.01.008

[12] A. Si-Ammour, S. Djennoune, M. Bettayeb, A sliding mode control for linear fractional systems with input and state delays, Communications in Nonlinear Science and Numerical Simulation 14 (2009) 2310-2318. https://doi.org/10.1016/j.cnsns.2008.05.011

[13] A. Azami, S. V. Naghavi, R. D. Tehrani, M. H. Khooban, F. Shabaninia, State estimation strategy for fractional order systems with noises and multiple time delayed measurements, IET Sci. Meas. Technol. 11 (2017) 9-17. https://doi.org/10.1049/iet-smt.2016.0089

[14] J. Si, W. Jiang, Sliding mode control for fractional differential systems with state-delay, Chin. Quart. J. Math. 27(2012) 117-122.

[15] X. Li, S. Yurkovich, Sliding mode control of delayed systems with application to engine idle speed control, IEEE Trans. Cont. Syst. Tech. 9 (2001) 802-810.

[16] S. Balochian, A. K. Sedigh, A. Zare, Stabilization of multi-input hybrid fractional-order systems with state delay, ISA Transactions 50 (2011) 21-27. https://doi.org/10.1016/j.isatra.2010.10.007

[17] P. Lanusse, H. Benlaoukli, D. Nelson-Gruel, A. Oustaloup, Fractional-order control and interval analysis of siso systems with time-delayed state, IET Control Theory Appl. 2 (2008) 16-23. https://doi.org/10.1049/iet-cta:20060491

[18] Z. H. Wang, Y. G. Zheng, The optimal form of the fractional-order difference feedbacks in enhancing the stability of a sdof vibration system, Journal of Sound and Vibration 326 (2009) 476-488.

[19] R. Behinfaraz, M. Badamchizadeh, A. R. Ghiasi, An adaptive method to parameter identification and synchronization of fractional-order chaotic systems with parameter uncertainty, Appl. Math. Model. 40 (2016) 4468-4479.

[20] Z. Gao, X. Lin, Y. Zheng, System identification with measurement noise compensation based on polynomial modulating function for fractional-order systems with a known time-delay, ISA Transactions 79 (2018) 62-72. https://doi.org/10.1016/j.isatra.2018.04.012

[21] Y. Dai, Y. Wei, Y. Hu, Y. Wang, Modulating function-based identification for fractional order systems, Neurocomputing 173 (2016) 1959-1966. http://dx.doi.org/10.1016/j.neucom.2015.07.002

[22] K. Kothari, U. Mehta, J. Vanualailai, A novel approach of fractional-order time delay system modeling based on Haar wavelet, ISA Transactions 80 (2018) 371-380. https://doi.org/10.1016/j.isatra.2018.07.019

[23] K. Kothari, U. Mehta, V. Prasad, J. Vanualailai, Identification scheme for fractional Hammerstein models with the delayed Haar wavelet, IEEE/CAA journal of automatica sinica 7 (2020) 1-10. https://doi.org/10.1109/JAS.2020.1003093

[24] Y. Tang, H. Liu, W. Wang, Q. Lian, X. Guan, Parameter identification of fractional order systems using block pulse functions, Signal Process. 107 (2015) 272-281.

[25] Lu, Y. Tang, X. Zhang, S. Wang, Parameter identification of fractional order systems with nonzero initial conditions based on block pulse functions, Measurement 158 (2020). https://doi.org/10.1016/j.measurement.2020.107684

[26] V. Prasad, U. Mehta, Modeling and parametric identification of Hammerstein systems with time delay and asymmetric dead-zones using fractional, differential equations, Mechanical Systems and Signal Processing 167 (2022). https://doi.org/10.1016/j.ymssp.2021.108568

[27] M.-H. Sin, C. Sin, S. Ji, S.-Y. Kim, Y.-H. Kang, Identification of fractional-order systems with both nonzero initial conditions and unknown time delays based on block pulse functions, Mechanical Systems and Signal Processing 169 (2022). https://doi.org/10.1016/j.ymssp.2021.108646

[28] Myong-Hyok Sin, Chol Min Sin, Hyang-Yong Kim, Yong-Min An, Kum-Song Jang, Parameter identification of fractional-order systems with time delays based on a hybrid of orthonormal Bernoulli polynomials and block pulse functions, Nonlinear Dyn (2024) 112: 15109-15132. https://doi.org/10.1007/s11071-024-09703-8

[29] M. Yi, J. Huang, J. Wei, Block pulse operational matrix method for solving fractional partial differential equation, Appl. Math. Comput. 221 (2013) 121-131. http://dx.doi.org/10.1016/j.amc.2013.06.016

[30] M. Behroozifar, S. Yousei, Numerical solution of delay differential equations via operational matrices of hybrid of block-pulse functions and Bernstein polynomials, Comput. Methods Diff. Eq. 1 (2013) 78-95.

[31] J. J. More, The Levenburg-Marquardt Algorithm: Implementation and Theory, Springer-Verlag, New York, 1977.

[32] G. Golub, V. Pereyra, The differentiation of pseudo-inverses and nonlinear least squares problems whose variable seperate, SIAM J. Numer. Anal. 10 (1973) 413-432. http://www.jstor.org/stable/2156365

[33] L. Kaufman, A variable projection method for solving separable nonlinear least squares problems, BIT 15 (1975) 49-57.